Towards energy-autonomous cities using CO_2 networks and Power to Gas storage

Raluca Suciu[a], Paul Stadler, Araz Ashouri and François Maréchal

[a] Ecole Polytechnique Fédérale de Lausanne (EPFL), Lausanne, Switzerland.
raluca-ancuta.suciu@epfl.ch, paul.stadler@epfl.ch, ashouri@alumni.ethz.ch, francois.marechal@epfl.ch

Abstract:

Under Energy Strategy 2050, the federal government of Switzerland plans to greatly reduce per capita energy consumption, decrease the share of fossil fuels, and replace the nuclear electricity generation by gains in efficiency and use of renewable energy sources. This work investigates the feasibility of defined goals through both the improvement of the efficiency of current energy systems and the increase in renewable energy sources.

For efficiency improvement, a new district energy network is proposed. District heating and cooling networks - usually use centralized, energy efficient conversion technologies based on water networks, which is not suitable for multi-temperature supply and heat recovery.

This work investigates a network using CO_2 as a refrigerant for heat transfer. The system utilizes the latent heat of vaporization as the main source of storage and transfer of heat, and allows for recovery of waste heat from cooling in heating, due to the two-pipe system.

This study also investigates the potential of this CO_2 network when coupled with renewable energy sources to satisfy the heating, cooling, and electricity requirements of urban areas in Switzerland.

Keywords:

CO_2 networks, district heating and cooling, renewable energy sources, self-sufficiency, urban energy systems

1. Introduction

Under Energy Strategy 2050, the federal government of Switzerland plans to greatly reduce per capita energy consumption, decrease the share of fossil fuels, and replace the nuclear electricity generation by gains in efficiency and use of renewable energy. The intrinsic stochastic behavior of this increasing share of renewable energies leads to a need for energy storage systems. While a portion of the demand for storage can be satisfied by battery stacks, they are spacious, expensive, and self-discharging, which makes them unsuitable for long-term energy storage. Therefore, it is of high interest to integrate an alternative storage method into the system.

Among the candidates, power-to-gas (P2G) is an established possibility for the conversion of electricity into a chemical energy carrier, namely methane. Methane production is an alternative worth investigating since the production process is well known at industrial level and the CO_2 emissions are low. This study is concerned with the investigation and optimization of the design and operation of P2G systems for the storage of renewable energy and bi-directional interaction with the electric grid. The system is mainly composed of PV panels, a high or low temperature (co-) electrolizer (solid oxide electrolysis cell (SOEC)), and a methane production and liquefaction system. The CO_2 district heating network (DHN) and the methane network complement the system. When methane is used, the P2G system has the potential to reach a round-trip efficiency of more than 60% [1, 2]. Furthermore, the integration of secondary technologies such as solid oxide fuel

Nomenclature

Acronyms

COP	Coefficient of performance
CP	Central plant
DHN	District heating network
ERA	Energy reference area
EV	Electrical vehicles
GT	Gas turbine
GW	Geothermal wells
HTE	High temperature electrolizer
LHV	Lower heating value
LTE	Low temperature electrolizer
MCFC	Molten carbon fuel cell
MPC	Model predictive control
NPV	Net present value
P2G	Power to gas
SOC	State of charge
SOEC	Solid oxide electrolysis cell
SOFC	Solid oxide fuel cell
YDD	Yearly degree days

Symbols

A	Area, m^2
C	Capacity, kW
$\dot{E}$	Electric power, W
g	Gravitational acc., kg m s^{-2}
h	Depth, m
I	Solar irradiation, W m^{-2}
$\dot{m}$	Mass flow kg s^{-1}
$\dot{Q}$	Heat rate, W
T	Temperature, K
T_{LM}	Logarithmic mean temperature difference, K
U	Heat transfer coefficient W m^{-2} K
$\dot{W}$	Geothermal energy, W m^{-1}

Greek Symbols

η	Efficiency
ΔT	Temperature change, K

Subscripts

a	Ambient
ch	Charging
$cond$	Condenser
CP	Central Plant
dch	Discharging
dhw	Domestic hot water
ERA	Energy reference area
$evap$	Evaporator
$geoth$	Geothermal
$glass$	Glass
$ground$	Ground level
gw	Geothermal well
hp	Heat pump
in	Flow in
LM	Logarithmic mean
NG	Natural gas
out	Flow out
PV	Photovoltaic panel
ref	Reference
$refr$	Refrigeration
SH	Space heating
sun	Sun
var	Varying
$water$	Water

cells (SOFCs) allows the system to reach even higher efficiencies by using waste heat from the electricity storage to supply heating or cooling via the CO_2 DHN. The benefits of the innovative advanced electricity storage will be demonstrated in the perspective of the future Swiss electric grid.

The increasing demand of electricity and the need to decrease fossil fuel consumption also requires the development of alternative power generation systems with higher efficiencies and lower environmental impact. An attractive solution for the energy conversion of fossil or bio-fuels is the cogeneration of heat and power. However, the existing systems have a number of drawbacks, such as high maintenance costs, low electrical efficiencies, vibrations and noise. Molten Carbon Fuel Cells (MCFC) and SOFCs have emerged as ideal candidates for decentralized electricity production. However, the fuel cell cannot completely convert the fuel electrochemically, and thus the remaining fuel is combusted after the fuel cell, typically with low energy efficiency. One solution for the improvement of the electrical efficiency is to combine the fuel cell with a gas turbine (GT) in a hybrid system, which takes advantage of the high operating temperature of the SOFC required to valorize the fuel.

Several studies investigated the SOFC feasibility and operating conditions and proposed design alternatives. Examples include the U.S. Department of Energy High Efficiency Fossil Power Plant,

who presented a low cost SOFC-GT system of 220kWe, which could achieve an efficiency of 60% [3]. *Massardo* and *Magistri* looked at pressurized and atmospheric pressure SOFCs with efficiencies between 65% and 75% [4]. *Facchinetti* et al. proposed a new hybrid cycle based on an inverted Brayton-Joule cycle, in which a solid oxide fuel cell operating under atmospheric pressure is combined with a gas turbine. This innovative system reaches an energy conversion efficiency of 83% and an exergy efficiency of 82.5% [5]. Further improvement is expected if an intercooled compressor is used in the anodic gas turbine.

An important part of the system is the hydrogen production. Intensive research efforts are necessary in order to find a suitable technology to supply hydrogen in large amounts and at a low price. The current production methods such as steam reforming, gasification of coal, or partial oxidation of heavy hydrocarbons require the use of fossil fuels. Other methods used for hydrogen production are electrochemical processes like photo-electrochemical methods, thermochemical water splitting or water electrolysis. Among them, water electrolysis is the only one commercially available at the moment. Based on their operating temperature, SOECs can be classified in low temperature electrolyzers (LTE) and high temperature electrolyzers (HTE). LTEs are proven technologies, which can achieve energy efficiencies of about 75% [6]. For HTEs, *M.A. Laguna* reported hydrogen production efficiencies of 50−95% at 900°C [7], while *Martinez-Fras* et al. showed that their system could reach up to 70% efficiency based on the primary energy and up to 90% efficiency based on the total energy input in the SOEC [8, 9].

This paper combines the P2G energy storage concept described above with CO_2 based district energy systems and investigates the potential of this novel approach using a case study performed on an area in the city center of Geneva.

2. Modeling

District heating and cooling networks usually use centralized, energy efficient conversion technologies based on water networks [10]. However, the supply temperature of these networks is selected according to the consumer with the highest temperature demand, while other users are supplied at a temperature higher than their needs. Additionally, the use of two independent water loops in cases when both heating and cooling are required does not allow for the recovery of any heat discharged in the cooling network.

By implementing a network using CO_2 as heat transfer fluid, the system utilizes the latent heat of vaporization as main storage and heat transfer source. The network also allows for recovery of waste heat from cooling in heating, due to the two-pipe system. However, since the heat required for heating does not always match the waste heat discharged from cooling, a central plant is required in order to balance the network. The central plant exchanges heat with the environment, and is represented either as a lake or as geothermal wells. A more detailed description of the refrigerant based network that uses CO_2 as the heat transfer fluid is given by *Weber* and *Favrat* and possible energy services and corresponding conversion technologies for refrigerant based networks have been investigated by *Henchoz* et al. [11, 12, 13].

The area analyzed in the scope of this report is "Rues Basses" in downtown Geneva. Specific consumption data (i.e. energy reference area (ERA)) was provided by the Geneva cantonal office for energy [14]. Three types of buildings were considered (total ERA: 687800 m^2):

- Office buildings (60% of the ERA)
- Commercial buildings (23% of the ERA)
- Residential buildings (17% of the ERA).

The energy services considered in the study are the following:

- Space heating
- Air conditioning

- Hot water preparation
- Refrigeration (for commercial use)
- Cooling of data centers.

The yearly energy required for the various services was computed by *Henchoz* et al. [15] using the Swiss standards [16] and additional statistical urban data assessment methods [17]. The daily energy requirements were evaluated taking into account the effect of the varying atmospheric temperature on space heating and air conditioning demand, using the following formula:

$$Q_{ERA} = \frac{UA}{ERA} \cdot \int (T_{service} - T_a) dt \tag{1}$$

Q_{ERA} represents the yearly space heating demand per m^2 of ERA. The formula combines the effect of the different heat sources and heat sinks, and the heat transfer coefficient (UA/ERA) links the thermal energy flow to the temperature difference between the room and the ambient air. The model is also known as the energy-signature model [18]. The integral can be replaced by the yearly heating/cooling degree-days (YDD) and the transfer coefficient becomes:

$$\frac{UA}{ERA} = \frac{Q_{ERA}}{YDD} \tag{2}$$

Geneva is reported to have 2937 heating degree-days [19]. The value is given for a base temperature of 20°C and under the assumption that the space heating service stops when the average daily ambient temperature exceeds 12°C. Equivalently, the annual cooling degree-days is 384. The value assumes a base temperature of 18°C, and the method used for the calculation was the UKMO method [20].

The total annual energy requirement is 102.448GWh, 51.8% for heating and 49.2% for cooling demands. Figure 1 depicts the energy required for each service throughout the year on a monthly basis. The heating peak occurs in February at a load of 15.5 MW_{th}. The heating demand reaches its minimum in summer, when the only heating demand is the one for the domestic hot water preparation. The cooling peak occurs in August at a load of 16.95 MW_{th}. The energy required for domestic hot water preparation is assumed to be 0.5 MW_{th}. The cooling capacity for refrigeration and cooling of data centers is 0.5 MW_{th} and 1.24 MW_{th} respectively.

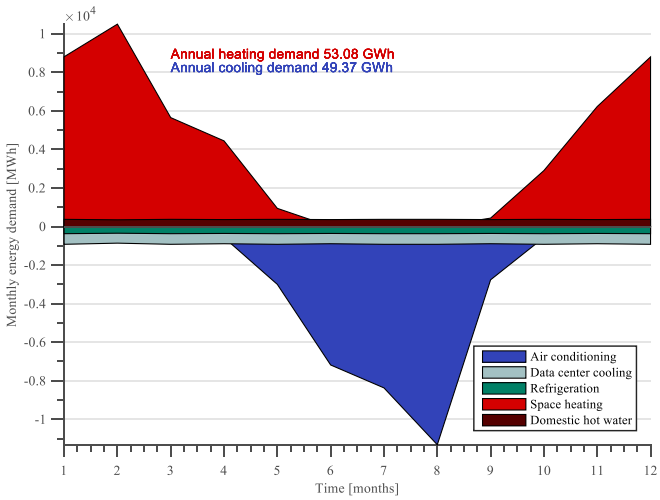

Fig. 1. *Energy demand for the area studied over the year 2012.*

The decentralized energy conversion technologies chosen to supply the energy services at the user end are (Figure 2):

- Heat pumps for space heating and domestic hot water. (The heat from the CO_2 condensation is

transferred to the refrigerant through a condenser-evaporator)

- Heat exchangers for air conditioning and data center cooling
- CO_2 vapor compression chillers for refrigeration. Liquid CO_2 is expanded from the network to the required saturation temperature and evaporated; the vapor produced is then recompressed and sent back to the network.

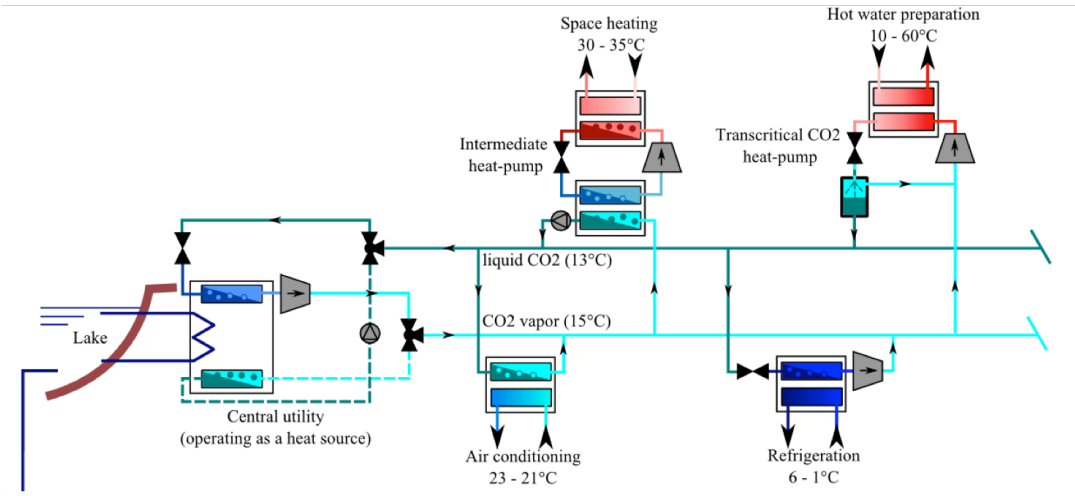

Fig. 2. *Schematic representation of a CO_2 based district energy network [15]*

The network has an annual energy consumption of 17.71 GWh. The electrical power has a peak in February at 5.23 MW. The minimum load occurs in summer, when space heating is not required and the central plant works in dissipation mode. The end user heat pumps account for the largest share of electricity required with 73.3%, the central plant is the second consumer with 25.1%, and the refrigeration accounts for 1.6%. Air conditioning and data center cooling are not on the graph, since they are provided through free cooling. Figure 3 shows the yearly electricity consumption on a monthly basis.

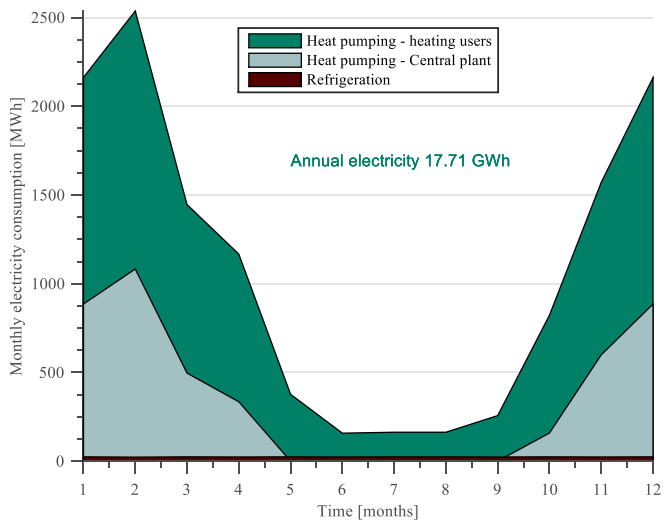

Fig. 3. *Electricity consumption for the CO_2 DHN over the year 2012*

The network is balanced using a central plant that exchanges heat with a nearby lake, through heat pumping or direct cooling. The connection to the lake is considered to be deep enough such that its temperature can be assumed to be constant throughout the year, at 7.5°C. The pressure of the CO_2 DHN is selected such that the saturation temperature in the vapor state is around 15°C, i.e. 50 bar. The temperature of the network is constrained by the desire to supply air conditioning and cooling of data centers via free cooling. This condition also results in a slightly higher pressure in the liquid

line as compared to the vapor one (of approx. 1 bar), in order to allow a natural flow of CO_2 in the heat exchangers used for free cooling.
In the following the system is described in detail, based on it's different energy technologies (heat pumps, SOEC/SOFC cogeneration unit), energy sources (PV panels, geothermal wells), the storage units available, and its interaction with the electrical grid.

2.1. Heat pumps

The coefficients of performance (COPs) of the different cycles were computed assuming a heat pump efficiency of $\eta_{hp} = 0.4$[21], and minimum temperature differences in the heat exchangers according to $\Delta T_{water-refr} = 1.5°C$, $\Delta T_{water} = 4°C$, $\Delta T_{refr-refr} = 1°C$ [15]. The evaporation/condensation temperatures of the heat pumps were computed using the demand temperature of the different services (Figure 2) and the minimum temperature differences. Their values are shown in Table 1 below.

Table 1. Parameters for heat pumps

Heat Pump	*Parameter*	*Value*	*Unit*	Heat Pump	*Parameter*	*Value*	*Unit*
Space heating	T_{evap}	285	K	Refrigeration	T_{evap}	268.5	K
	T_{cond}	313.5	K		T_{cond}	286	K
Domestic hot water	T_{evap}	286-288	K	Central plant	T_{evap}	276	K
(transcritical HP)	T_{cond}	343-353	K		T_{cond}	289	K

The COPs of the heating pumps were computed according to:

$$COP_{CP} = COP_{SH} = \eta_{hp} \cdot \frac{T_{cond}}{T_{cond} - T_{evap}} \tag{3.1}$$

$$COP_{refr} = \eta_{hp} \cdot \frac{T_{evap}}{T_{cond} - T_{evap}} \tag{3.2}$$

$$COP_{dhw} = \eta_{hp} \cdot \frac{T_{LM,cond}}{T_{LM,cond} - T_{LM,evap}} \tag{3.3}$$

where the logarithmic mean temperature difference is:

$$T_{LM,ab} = \frac{T_a - T_b}{ln\frac{T_a}{T_b}} \tag{4}$$

The energy requirement of the energy conversion technologies is satisfied using PV panels, energy from the grid (i.e. the renewable share from the Swiss Energy Mix for 2050, for the specific ERA [22]), electricity and heat from the SOFC, and energy from the environment (provided by a lake or by geothermal wells). A schematic description of the different units and streams of the process is shown in Figure 4.

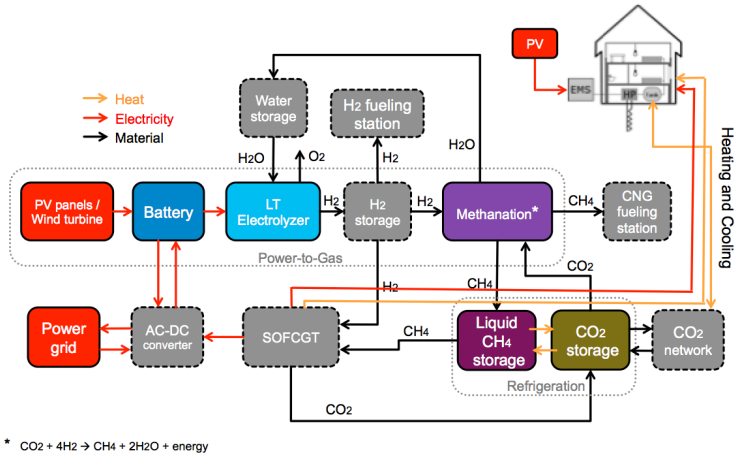

Fig. 4. *Advanced CO_2 based district energy network*

2.2. PV panels

The PV was modeled as described in [23], with η_{PV} the PV efficiency, I_{sun} the irradiation of the sun, T_{PV} the PV temperature, U_{glass} the thermal transmission coefficient, and f_{glass} the factor denoting the portion of the solar irradiation passing through the PV glass:

$$E_{PV,out} = A_{PV} \cdot \eta_{PV} \cdot I_{sun} \tag{5.1}$$

$$\eta_{PV} = \eta_{PV,ref} - \eta_{PV,var} \cdot \left(T_{PV} - T_{PV,ref}\right) \tag{5.2}$$

$$T_{PV} = \frac{U_{glass} \cdot T_a}{U_{glass} - \eta_{PV,var} \cdot I_{sun}} + \frac{I_{sun} \cdot \left(f_{glass} - \eta_{PV,ref} - \eta_{PV,var} \cdot T_{PV,ref}\right)}{U_{glass} - \eta_{PV,var} \cdot I_{sun}} \tag{5.3}$$

The different parameters assumed are given in Table 2 [23].

Table 2. Parameters for the PV panel

Parameter	*Value*	*Unit*	Parameter	*Value*	*Unit*
T_a	288	K	f_{glass}	0.9	-
$T_{PV,ref}$	298	K	$\eta_{PV,ref}$	0.14	-
U_{glass}	29.1	W/m^2	$\eta_{PV,var}$	0.001	-

The price of the PV was estimated at 750 €/m^2 [23], with an annual operation and maintenance cost of 22.15 €/m^2 [24].

2.3. SOEC-SOFC cogeneration unit

The efficiencies for the SOEC-SOFC cogeneration unit were set to 75% and 18% for the electrical and thermal efficiency of the SOFC and 78% for the electrical efficiency of the SOEC. Other parameters used for the cogeneration unit were the lower heating value of natural gas $LHV_{NG} = 43000\ kJ/kg$ and the heat of evaporation of carbon dioxide $L_{CO_2} = 374\ kJ/kg$ [25]. The waste heat of the SOFC was set to 80°C and was used for both space heating and hot water preparation.

The cost of the SOEC-SOFC cogeneration unit was calculated under the assumption that it must be competitive on the market, and therefore its price should be comparable to other cogeneration heat and power units of the same size [26].

2.4. Storage tanks

The storage tanks were modeled using the following equations:

$$C_{tank} \cdot SOC_{tank}(k+1) = C_{tank} \cdot SOC_{tank}(k) + \eta_{ch} \cdot \dot{m}_{fuel,in} - \frac{1}{\eta_{dch}} \cdot \dot{m}_{fuel,out} \quad (6.1)$$

$$SOC_{tank}(k) \in [0,1]\ \forall k \quad (6.2)$$

where $SOC_{tank}(k)$ represents the state of charge of the tank at time step k, C_{tank} the tank capacity, and $\eta_{ch} = \eta_{dch} = 0.95$ the charging and discharging efficiencies. The CO_2 is stored in liquid form at the operating network pressure and temperature of 50 bars and 13°C, respectively. The methane is also stored as a liquid, at the operating pressure of 1 bar and the corresponding temperature required for the liquid state, of -162°C. Their corresponding densities at these pressures and temperatures are 839.97 kg/m^3 for CO_2 and 423.19 kg/m^3 for CH_4. The economic evaluation was done based on the cost functions provided by *G.D.Ulrich* et al. and *R. Turton* et al. [27, 28].

2.5. Geothermal wells

For the analysis of the geothermal wells, the calculation was based on the work of *F. Amblard* et al. [29]. The parameters used are listed in Table 3 below:

Table 3. Parameters for geothermal wells

Parameter	*Value*	*Unit*
geothermal gradient (z_{geoth})	303	K/km
temperature of the ground (T_{ground})	283	K
geothermal energy ($\dot{W}_{geoth}$)	60	W/m
temperature of evaporation (T_{evap})	286	K

The electricity needed for pumping in the geothermal wells $\dot{E}_{gw}$ was computed according to:

$$\dot{E}_{gw} = \frac{\dot{m}_{CO_2} \cdot g \cdot h}{\eta_{geoth}} \quad (7.1)$$

with g the gravitational acceleration, $\dot{m}_{CO_2}$ the mass flow of CO_2, η_{geoth}=0.8 the geothermal pump efficiency [30], and h the depth of the geothermal well, given by:

$$h = \frac{T_{evap} - T_{ground}}{z_{geoth}} = 166.67m \quad (7.2)$$

The number of geothermal wells required was found using:

$$N_{GW} = \frac{\dot{Q}_{GW}}{h \cdot \dot{W}_{geoth}} \quad (7.3)$$

with $\dot{Q}_{GW}$ the heat provided by the geothermal well. The cost analysis was also based on the data provided in [29].

2.6. Grid interaction and electrical vehicles (EV)

It is also necessary to consider the energy demand of the utilities inside the house and of electrical cars. The electricity needed for the utilities was estimated using the average electricity needed per square meter of ERA (80 MJ/m^2 [31]), while the electricity requirement for the electrical cars was calculated using the parameters presented in Table 4.

Table 4. Parameters for electricity demand of electrical cars

Parameter	*Value*	*Unit*
area/inhabitant	40	m^2
inhabitants/car	2	-
distance/car	20000	km/year
electricity	0.25	kWh/km

3. Results and discussion

The results are divided in 2 categories, based on the source that provides the heat from the environment:

a) The heat from the environment provided by lake Léman (Geneva) (central plant (CP));
b) The heat from the environment provided by geothermal wells (GW).

Within these two cases, four subcases will be discussed:

1. Heating, cooling and utility requirements are considered;
2. Heating, cooling and utility requirements are considered, and the share of renewable energy from the Swiss Energy Mix for 2050 is taken into account;
3. Heating, cooling, utility requirements, and electrical cars are considered;
4. Heating, cooling, utility requirements, and electrical cars are considered and the share of renewable energy from the Swiss Energy Mix for 2050 is taken into account.

First, an analysis of the PV panel area required in each case is performed. The base case assumes all of the electricity is supplied by PV panels, and the system is allowed to sell electricity to the grid. In this case the PV panel area required 1184922 m^2 and PV panel area/ERA is 1.723. The other cases include the SOFC-SOEC cogeneration and vary according to the criteria a) - b) and 1 - 4 as explained above. The different PV panel areas and PV panel areas per squared meter of ERA for these different cases are illustrated in Figure 5 and the grid interaction in Figure 6 (the cases which are not present in the figure had no power drawn from the grid

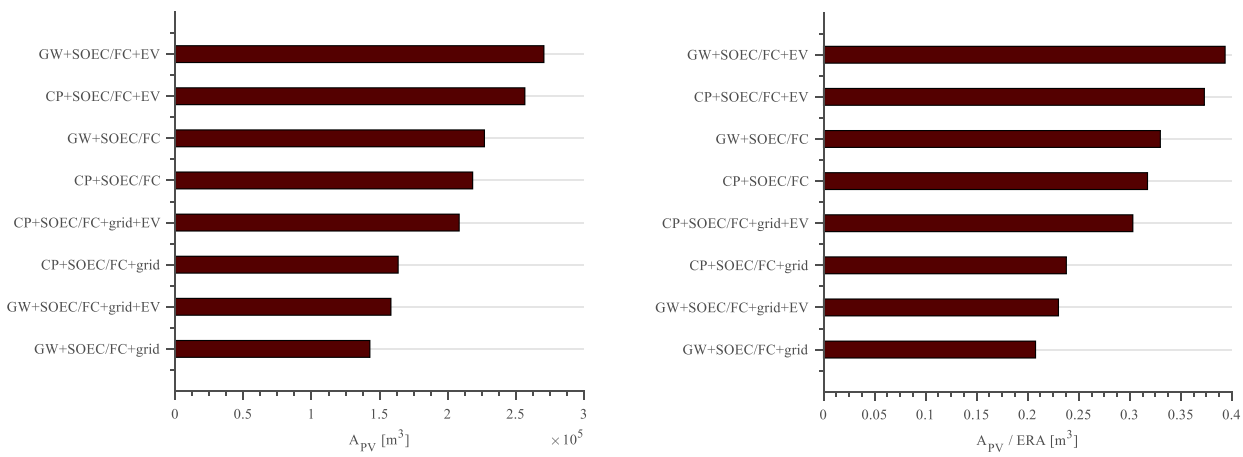

Fig. 5. *PV panel area (left) / PV panel area per ERA (right) for different cases*

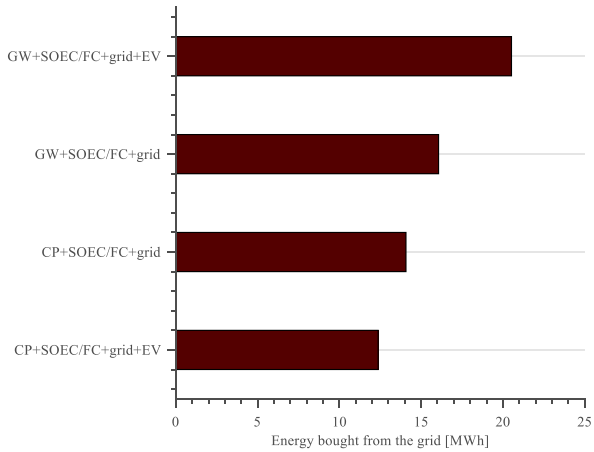

Fig. 6. *Energy bought from the grid for different cases*

The PV panel area decreases in the case of an open system (i.e. the renewable energy mix is included) since the PV load is reduced. When the electricity required for the electrical cars is considered, the PV panel area required is higher, due to the higher demand. The area of the PV panels required to satisfy the different urban demands (a) in addition to the use of electrical cars (b) decreases by 25.1% (a) and 18.8% (b) respectively when adding the renewable share of the Swiss electricity mix and using the lake, and by 37.1% and 41.5% when using geothermal wells. Regarding the feasibility of the system, the base case scenario is deemed infeasible here, because the rooftop area of the buildings would not be enough for the PV panels, even if only 1-floor buildings are considered. However, when the cogeneration unit is included, the rooftop area would be sufficient if building as low as 3-4 floors are included.

Table 5 shows the energy requirement of the heat pumps for each case.

Table 5. Energy demand of the central plant and user end heat pumps for different cases

Case nr.	*Case*	E_{HP} *[GWh]*	$E_{HP,\ CP}$ *[GWh]*	$E_{HP,\ users}$ *[GWh]*
1. a)	CP+SOEC/FC	16.30	4.09	12.21
2. a)	CP+SOEC/FC+grid	16.68	4.20	12.28
3. a)	CP+SOEC/FC+EV	16.17	4.05	12.12
4. a)	CP+SOEC/FC+grid+EV	16.58	4.17	12.41
1. b)	GW+SOEC/FC	12.79	3.96	8.83
2. b)	GW+SOEC/FC+grid	13.02	4.01	9.01
3. b)	GW+SOEC/FC+EV	12.71	3.94	8.77
4. b)	GW+SOEC/FC+grid+EV	12.85	3.98	8.87

The energy demand of the central plant heat pump decreases when the geothermal wells are used, as more heat is extracted from the environment for the same demand. Thus, most of the electricity required in the first stage, which accounts for 25% of the total demand, is saved. Next, the number of geothermal wells required to replace the central plant was computed for the 4 different cases. The results are shown in Table 6 below.

Table 6. Number of geothermal wells required for different cases

Case nr.	*Case*	N_{GW}
1. b)	GW+SOEC/FC	1632
2. b)	GW+SOEC/FC+grid	1634
3. b)	GW+SOEC/FC+EV	1630
4. b)	GW+SOEC/FC+grid+EV	1635

A number of approximately 1630 geothermal wells are required to replace the central plant. The different sizes required for the CO_2 and CH_4 storage tanks can be observed in Table 7 below.

Table 7. CO_2 and CH_4 storage tank sizes

Case nr.	*Case*	V_{CH4} *[m³]*	V_{CO2} *[m³]*	V_{CH4} *[m³/(4 hab)]*	V_{CO2} *[m³/(4 hab)]*
1. a)	CP+SOEC/FC	3655	4560	5.00	6.24
2. a)	CP+SOEC/FC+grid	2497	3116	3.42	4.26
3. a)	CP+SOEC/FC+cars	4057	5061	5.55	6.93
4. a)	CP+SOEC/FC+grid+cars	2822	3520	3.86	4.82
1. b)	GW+SOEC/FC	2756	3439	3.77	4.71
2. b)	GW+SOEC/FC+grid	1851	1178	2.53	1.61
3. b)	GW+SOEC/FC+cars	3115	3886	4.26	5.32
4. b)	GW+SOEC/FC+grid+cars	2360	3263	3.23	4.46

The sizes of the storage tanks are smaller for the cases in which geothermal wells are used, as the overall energy demand is lower. Moreover, the volumes of the storage tanks required are less than 5.55 m^3/(4 hab) for CH_4 and 6.93 m^3/(4 hab) for CO_2, which are both far smaller than the volume of a battery that would be required for a self-sufficient house (with 4 inhabitants), of 163m^3 [32].

Next, a comparative profitability analysis is performed. The performance indicator chosen is net present value (NPV). NPV is an indicator that shows the difference between the present value of future cash flows from an investment and the amount of investment. The present value of the expected cash flows is computed by discounting them using a fixed interest rate. The NPV for every year of operation is computing considering:

- The initial investment
- The revenues due to the savings in the cost of buying electricity from the grid
- The revenues due to the cost of selling electricity to the grid
- The cost of replacing the equipment
- The cost of operation and maintenance

The price of electricity bought from and sold to the grid is set to 0.2 €/kWh and 0.1 €/kWh, respectively. The price for the electricity from the renewable energy mix was assumed to be the same as the price of electricity bought from the grid, 0.2 €/kWh, and the price of heating and cooling services was set to 0.108 €/kWh [15].

For this analysis, a lifetime of 39 years was considered corresponding to the lifetime of pipes, while the rest of the equipment was assumed to have a lifetime of 20 years. Therefore, one replacement of equipment was taken into account during the chosen lifetime. The PV panel price was varied between 750 €/m^2 and 300 €/m^2 and the interest rate between 0.01 and 0.07. The results can be observed in Figure 7.

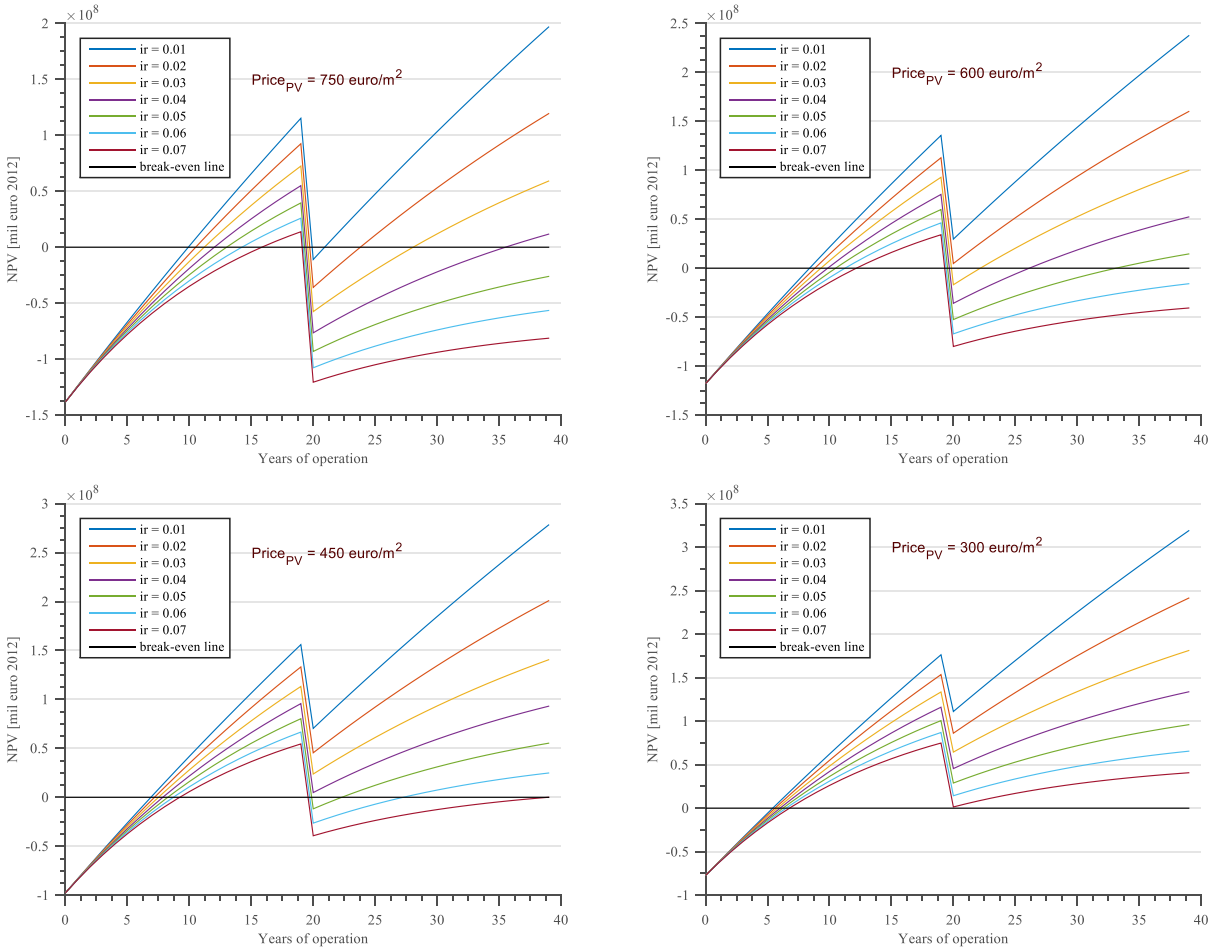

Fig. 7. *NPV for different PV prices and different interest rates*

The profit (i.e. NPV after 39 years) decreases with increasing interest rate, while the break-even period increases with increasing interest rate. For a PV of 750 €/m^2 the first break-even is achieved after 16 years for the highest interest rate, while the break-even after the replacement of the equipment is not achieved for interest rates higher than 0.04. When the PV price is set to 600 €/m^2, the first break-even is achieved after 13 years for the highest interest rate and the break-even after the replacement of the equipment is not achieved for interest rates higher than 0.05. For PV prices of 450 €/m^2 or 300 €/m^2 the first break-even for the highest interest rate occurs after 10 and 7 years respectively, and the second break-even is achieved for all interest rates.

4. Conclusions

The energy required for space heating, domestic hot water, air conditioning, refrigeration and data center cooling was evaluated on a monthly basis for the area "Rues Basses" in Geneva. The annual energy demand is 102.45 GWh, 51.8% related to heating and 41.2% to cooling services. Several cases have been considered based on the system specific heat source, electricity supply and service provision.

This study analyzed the integration of PV panels and SOEC-SOFC combined heat and power units to provide the required power demands. It has been shown that the area of the PV panels required to satisfy the different urban power requirements (case a) in addition to the use of electrical vehicles (case b) decreases by 25.1% and 18.8% respectively, when adding the renewable share of the Swiss electricity mix and using the lake, and by 37.1% and 41.5% respectively, when using geothermal wells.

The energy demand of the heat pumps was compared for the different cases; the power requirements of the central plant decreases when integrating geothermal wells since more heat is extracted from the environment for the same demand. The number of geothermal wells required to entirely replace the central plant is of 1635. In addition, the different sizes of the storage tanks required for each scenario were compared to the case of a battery stack related to a net zero energy building of 4 inhabitants; the respective volumes of 5.55 m^3/(4 hab) for CH_4 and 6.93 m^3/(4 hab) for CO_2 are much smaller than the one of the battery, of 163 m^3/(4 hab).
The NPV sensitivity analysis was done for PV prices between 750 €/m^2 and 300 €/m^2 and interest rates between 0.01 and 0.07. The profit decreased with increasing interest rate, while the break-even period increased with increasing interest rate. The different break even times for the highest interest rates for PV prices of 750, 600, 450 and 300 €/m^2 were 16, 13, 10, and 7 years respectively.
Future work includes a feasibility analysis for the entire Switzerland. This will imply performing a cost analysis on the profitability of installing the system depending on the density of a specific area. The SOFC and SOEC units will be modeled in detail and integrated with the storage units through liquefaction/evaporation processes. The possibility for heat recovery will be explored further in view of upgrading the environment heat and saving the first stage compression power. The option of integrating Model Predictive Control (MPC) in the system will be explored in order to further improve the system performance.

References

[1] Quaschning, V. (2013). Regenerative Energiesysteme: Technologie, Berechnung, Simulation. 8., aktual. ed.

[2] Jensen, S. H., Graves, C., Mogensen, M., Wendel, C., Braun, R., Hughes, G., ... & Barnett, S. A. (2015). Large-scale electricity storage utilizing reversible solid oxide cells combined with underground storage of CO 2 and CH 4. *Energy & Environmental Science*, *8*(8), 2471-2479.

[3] Lundberg, W. L., Veyo, S. E., & Moeckel, M. D. (2003). A high-efficiency solid oxide fuel cell hybrid power system using the Mercury 50 advanced turbine systems gas turbine. *Journal of Engineering for Gas Turbines and Power*, *125*(1), 51-58.

[4] Massardo, A. F., & Magistri, L. (2001, June). Internal Reforming Solid Oxide Fuel Cell Gas Turbine Combined Cycles (IRSOFC-GT): Part B—Exergy and Thermoeconomic Analyses. In *ASME Turbo Expo 2001: Power for Land, Sea, and Air* (pp. V002T04A015-V002T04A015). American Society of Mechanical Engineers.

[5] Facchinetti, E., Favrat, D., & Maréchal, F. (2011). Innovative Hybrid Cycle Solid Oxide Fuel Cell-Inverted Gas Turbine with CO2 Separation. *Fuel Cells*, *11*(4), 565-572.

[6] Dönitz, W., & Streicher, R. (1980). Hochtemperatur-Elektrolyse von Wasserdampf–Entwicklungsstand einer neuen Technologie zur Wasserstoff-Erzeugung. *Chemie Ingenieur Technik*, *52*(5), 436-438.

[7] Laguna-Bercero, M. A. (2012). Recent advances in high temperature electrolysis using solid oxide fuel cells: A review. *Journal of Power Sources*, *203*, 4-16.

[8] Martinez-Frias, J., Pham, A. Q., & Aceves, S. M. (2003). A natural gas-assisted steam electrolyzer for high-efficiency production of hydrogen. *International Journal of Hydrogen Energy*, *28*(5), 483-490.

[9] Martinez-Frias, J., Pham, A. Q., & Aceves, S. M. (2001, November). Analysis of a high-efficiency natural gas-assisted steam electrolyzer for hydrogen production. In *American Society of Mechanical Engineers, International mechanical engineering congress and exposition, New York, NY*.

[10] Fazlollahi, Samira, et al. "Multi-objective, multi-period optimization of district energy systems: IV–A case study." *Energy* 84 (2015): 365-381.

[11] Weber, C., & Favrat, D. (2010). Conventional and advanced CO 2 based district energy

systems. *Energy*, *35*(12), 5070-5081.
[12] Henchoz, S., Weber, C., Maréchal, F., & Favrat, D. (2015). Performance and profitability perspectives of a CO 2 based district energy network in Geneva's City Centre. *Energy*, *85*, 221-235.
[13] Henchoz, S. (2011). On a Multi-service, CO2 Based, District Energy System for a Better Energy Efficiency of Urban Areas. In *WEC 2011* (No. EPFL-CONF-169243).
[14] Romanowicz R. Rapport détude - Reseau urbain de distribution de la chaleur et du froid employant le CO2 - Technical report. Geneva, Switzerland: Geneva's Cantonal Office for Energy, 2011.
[15] Henchoz, S., Weber, C., Maréchal, F., & Favrat, D. (2015). Performance and profitability perspectives of a CO 2 based district energy network in Geneva's City Centre. *Energy*, *85*, 221-235.
[16] Swiss standard SIA 565 380/1. Lénergie dans le bâtiment, SIA, Zürich. 1988 Switzerland.
[17] GirardinL.2012 [PhD.Thesis]. http://infoscience.epfl.ch/record/170535/files/EPFL_TH5287.pdf [accessed 13.04.15].
[18] Hammarsten, S. (1987). A critical appraisal of energy-signature models. *Applied Energy*, *26*(2), 97-110.
[19] Geneva's Cantonal Office for Statistics [internet]. Geneva, Switzerland: spreadsheet of monthly meteorological data and heating degree-days since 2000. Available at: www.ge.ch/statistique/tel/domaines/02/02_03/T_02_03_2_02.xls [accessed 04.07.14].
[20] Mourshed, M. (2012). Relationship between annual mean temperature and degree-days. *Energy and buildings*, *54*, 418-425.
[21] Stene, J. "Integrated CO_2 heat pump systems for space heating and hot water heating in low-energy houses and passive houses", International Energy Agency (IEA) Heat Pump Programme – Annex 32 (2007).
[22] Gironès, V. C., Moret, S., Maréchal, F., & Favrat, D. (2015). Strategic energy planning for large-scale energy systems: A modelling framework to aid decision-making. *Energy*, *90*, 173-186.
[23] Ashouri, Araz. Diss., Eidgenössische Technische Hochschule ETH Zürich, Nr. 21908, 2014.
[24] Fux, S. F. (2013). *Optimal energy management and component sizing of a stand-alone building energy system* (Doctoral dissertation, ETH).
[25] Aresta, Michele. *Reaction Mechanisms in Carbon Dioxide Conversion*. Eds. Angela Dibenedetto, and Eugenio Quaranta. Springer, 2015.
[26] Rubio-Maya, C., Uche-Marcuello, J., Martínez-Gracia, A., & Bayod-Rújula, A. A. (2011). Design optimization of a polygeneration plant fuelled by natural gas and renewable energy sources. *Applied Energy*, *88*(2), 449-457.
[27] Ulrich, G. D. (1984). *A guide to chemical engineering process design and economics* (p. 295). New York: Wiley.
[28] Turton, R., Bailie, R. C., Whiting, W. B., & Shaeiwitz, J. A. (2008). *Analysis, synthesis and design of chemical processes*. Pearson Education.
[29] Amblard, F. L. P. R. M. (2015). *Geothermal energy integration in urban systems. The case study of the city of Lausanne* (No. EPFL-STUDENT-208829).
[30] Self, Stuart J., Bale V. Reddy, Marc A. Rosen. "Geothermal heat pump systems: Status review and comparison with other heating options", Applied Energy 101 (2013): 341-348.
[31] European Communities 2002, "Energy consumption in the services sector", ISBN 92-894-3362-0.
[32] P. Stadler, A. Ashouri, F. Maréchal, "Model-based optimization of distributed and renewable energy systems in buildings", Energy & Buildings 120 (2016): 103-113.